

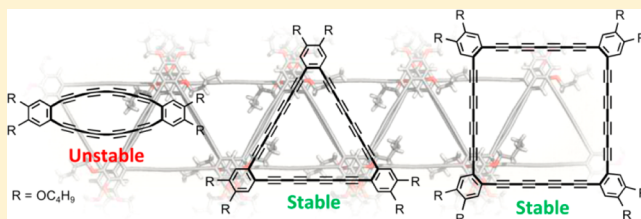
Hexadecadehydrodibenzo[20]-, Tetracosadehydrotribenzo[30]-, and Dotriacontadehydrotetrabenzo[40]annulenes: Syntheses, Characterizations, Electronic Properties, and Self-Associations

Shin-ichiro Kato, Nobutaka Takahashi, and Yosuke Nakamura*

Division of Molecular Science, Faculty of Science and Technology, Gunma University, 1-5-1 Tenjin-cho, Kiryu, Gunma 376-8515, Japan

Supporting Information

ABSTRACT: Hexadecadehydrodibenzo[20]-, tetracosadehydrotribenzo[30]-, and dotriacontadehydrotetrabenzo[40]-annulene derivatives ([20]-, [30]-, and [40]DBAs) possessing tetrayne linkages were synthesized. X-ray diffraction analysis demonstrated that the molecules of [30]DBA and *p*-xylene form a 2D sheetlike structure. Planar [20]- and [30]DBAs show significantly weak or almost no tropicity. The extension of the acetylenic linkages from a diyne to a tetrayne unit narrows HOMO–LUMO gaps. The self-association behavior of [30]DBA in solution resulting from effective π – π stacking interactions was observed.



INTRODUCTION

Acetylenic macrocycles, particularly dehydro[*n*]annulenes ([*n*]DAs) and dehydrobenzo[*n*]annulenes ([*n*]DBAs) in which *n* denotes the number of π electrons in the cyclic pathway, have received long-lasting attention in not only the basic aspect of aromaticity/antiaromaticity (namely, the tropicity of cyclic π -conjugated systems)¹ but also materials science because of their particularly interesting optoelectronic and self-assembling properties.² Because the Cu-mediated homocoupling reactions of ene-diyne or diethynylbenzenes, which are available with relative ease, have been well established, a variety of [*n*]DAs and [*n*]DBAs that consist of alkene or benzene moieties, respectively, and diyne linkages at the unsaturated bond were synthesized, including [12]DBA **1a**,³ [18]DBA **2a**,⁴ and their derivatives.² Moreover, advances in the field of Pd-catalyzed alkyne cross-coupling reactions have brought about the synthesis of related DBAs with more sophisticated functionality and the construction of larger and more complex DBA systems.⁵

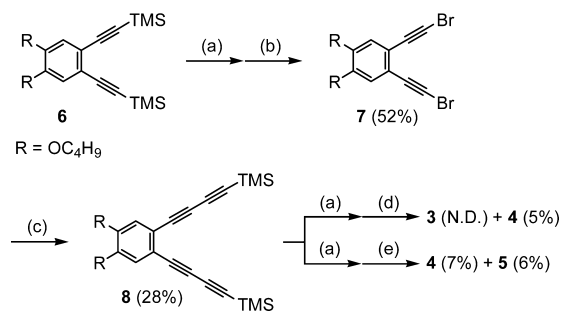
The incorporation of oligoyne linkages that are longer than diyne linkages into DA and DBA systems would allow us to obtain valuable insight into relevant structure–property relationships, namely, the effects of the ring expansion on the stability, tropicity, and electronic properties. However, examples of DAs and DBAs possessing oligoyne linkages are quite limited to date, and a summary of those in particular resulting from the groups of Haley,⁶ Tobe,⁷ and Diederich⁸ is included in Figure S1 in the Supporting Information. One of the reasons for the lack of [*n*]DAs and [*n*]DBAs possessing oligoyne linkages may be that acetylenic compounds become unstable with an increasing number of conjugated C \equiv C–C bonds.^{9,10} We describe herein the syntheses, characterizations, and properties of hitherto unknown hexadecadehydrodiben-

zo[20]-, tetracosadehydrotribenzo[30]-, and dotriacontadehydrotetrabenzo[40]annulene derivatives **3–5** possessing tetrayne linkages. By comparing the properties of **3–5** with those of [12]DBA **1b** and [18]DBA **2b**, we focused on the elucidation of the relationship between the ring size and the properties in the present DBA systems.

RESULTS AND DISCUSSION

Synthesis and Structures. The synthesis of DBAs **3–5** is outlined in Scheme 1. Compound **6** was converted into

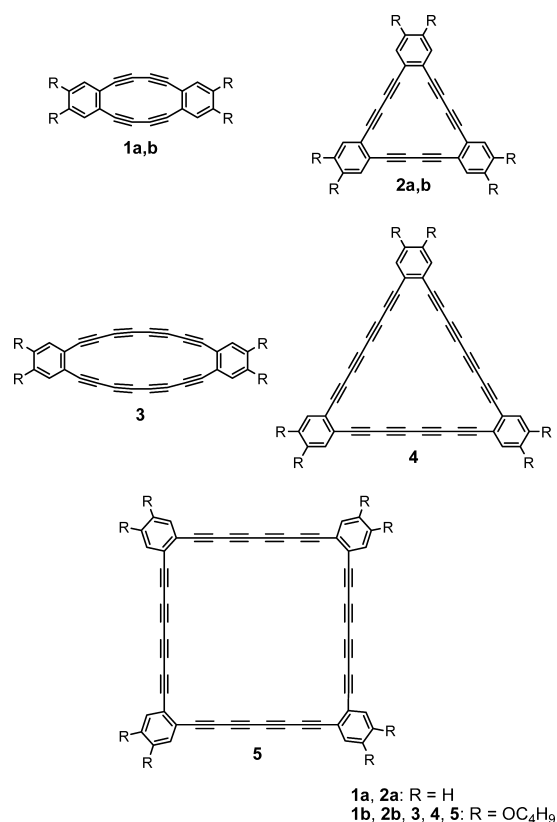
Scheme 1. Synthesis of [20]-, [30]-, and [40]DBAs **3–5**^a



^aReagents and conditions: (a) K₂CO₃, THF/MeOH (1:1), and rt. (b) AgNO₃, NBS, THF/MeOH (1:1), and rt. (c) CuCl, NH₂OH·HCl, *n*-BuNH₂, TMSA, CH₂Cl₂/H₂O (7:5), and 0 °C. (d) CuCl, TMEDA, acetone, and –5 °C to rt. (e) [PdCl₂(PPh₃)₂], CuI, *p*-benzoquinone, THF/Et₃N (1:2), and rt. TMSA = trimethylsilylacetylene. TMEDA = *N,N,N',N'*-tetramethylethylenediamine.

Received: June 8, 2013

Published: July 3, 2013



bromoalkyne **7** via desilylation with K₂CO₃ followed by silver-catalyzed bromination (52% in two steps). The Cadiot–Chodkiewicz coupling of **7** with trimethylsilylacetylene (TMSA) provided silyl-protected bisbutadiynyl arene **8** (28%). Desilylation of **8** with K₂CO₃ afforded the free alkyne that showed only limited stability in its neat form, which was rapidly placed under the Hay coupling condition in acetone. The careful separation of the crude mixture obtained in the macrocyclization afforded [20]DBA **3** and [30]DBA **4** (5% in two steps). The yield of **3** could not be determined because **3** could be handled only in solution; a neat sample rapidly polymerized to furnish black, intractable materials. The Pd-catalyzed coupling reaction was also investigated, and [40]DBA **5** (6%) and **4** (7%) were isolated. The low yields from the macrocyclization are probably due to the decomposition of the free alkyne during the reactions and/or the formation of oligomeric or polymeric products. Compounds **3–5** were undoubtedly identified by MS (FAB or MALDI–TOF) analysis together with their highly symmetric NMR spectra as described below. DBAs **4** and **5** showed higher stability than **3** and could be stored in the solid state at –15 °C for over a year. At room temperature, the solid sample of [30]DBA **4** gradually decomposed within a few months. However, [40]DBA **5** did not show any sign of decomposition when kept in the solid state for over a year. DBAs **1b** and **2b** were synthesized according to a literature procedure.^{11,12}

We calculated the molecular structures of [20]-, [30]-, and [40]DBAs **3'–5'** together with [12]DBA **1'** and [18]DBA **2'**, in which the butoxy groups in **1–5** were replaced with methoxy groups, at the B3LYP/6-31G* level of theory.¹³ Optimized structures **1'–4'** are planar (*D*_{2h} symmetry for **1'** and **3'**, *D*_{3h} symmetry for **2'** and **4'**). The structure of **5'** was calculated to be a nonplanar *D*_{2d}-symmetric structure (Figure S9). Unlike **2'**, **4'**, and **5'**, the C≡C–C bonds in **1'** and **3'** are apparently

deformed from linearity. The bending angles of the C≡C–C bonds in **3'** are 170.3–175.2°, whereas those in **1'** are 164.1–167.5°; thus, the strain in C≡C–C bonds in **3'** is predicted to be released in comparison to that of **1'**. The evidence for the moderate strain in the C≡C–C bonds of **3** is manifested by the downfield shifts of the ¹³C NMR peaks of the sp carbons by ca. 4 to 5 ppm for **3** compared to **4**. Nevertheless, **3** shows drastically reduced stability as compared to **1**. Although the reason for this finding is unclear at present, a similar severe instability in cyclic alkyl tetraynes was reported by Tykwinski and co-workers.¹⁴

Single crystals of **4** suitable for X-ray diffraction analysis were obtained by recrystallization from a *p*-xylene solution as a clathrate, with *p*-xylene having a 2:5 stoichiometry (Figure S2). The C≡C–C bond angles are 176.5–179.8°, and the deviation from the mean plane composed of the benzene moieties and tetrayne linkages is at most 0.205 Å. In the crystal lattice, the large cavity of **4** is occupied with a *p*-xylene molecule or the butoxy chain of the neighboring molecule. Interestingly, the molecules of **4** and *p*-xylene form a 2D sheetlike structure in which the [30]DBA cores roughly align within the plane (Figure 1).¹⁵

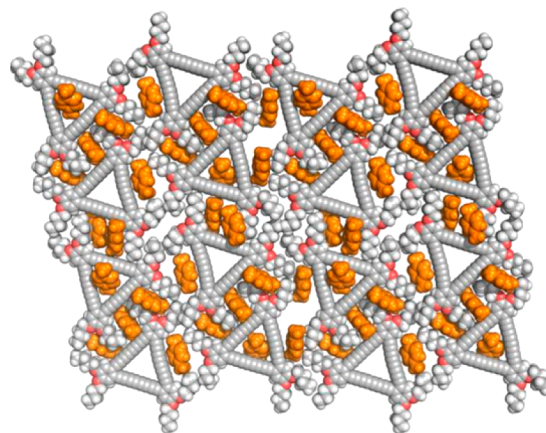


Figure 1. Packing structure of (DBA **4**)₂·(*p*-xylene)₅.

¹H NMR Spectra and NICS Calculations. DBAs **3–5** displayed very simple ¹H NMR spectra; thus, one singlet signal for aromatic protons was observed (Figures S17 and S18). Planar [20]- and [30]DBAs **3** and **4** are formally antiaromatic and aromatic, respectively. The change in resonance ($\Delta\delta$) of aromatic protons is a good indicator of the elucidation of tropicity. The signal of the aromatic protons for **3** is upfield shifted by $\Delta\delta = 0.28$ ppm with respect to the signal for acyclic **8**. The signal for **4** is only slightly downfield shifted by $\Delta\delta = 0.05$ ppm, which is almost comparable to the shift ($\Delta\delta = 0.02$ ppm) for nonplanar, apparently nonaromatic **5**. The observed chemical shift changes from acyclic **8** to **3** and **4** are apparently small as compared to those from **6** to **1b** and **2b**, respectively; the $\Delta\delta$ values are 0.51 ppm for **1b** and 0.20 ppm for **2b** with respect to **6**. This finding indicates that the tropicity of **3** and **4** substantially decreases as compared to corresponding **1b** and **2b** owing to the expansion of the dehydroannulene ring. Vollhardt and Matzger first reported the attenuating effect of the increase in the size of DBA rings on the NICS values.^{3b,16} Indeed, the NICS(0) (and NICS(1)) values of **3'** calculated at the GIAO/HF/6-31G*//B3LYP/6-31G* level are +1.14 (+1.07), which are only ca. 30% of those of **1'** (+3.84

(+3.70)); the NICS(0) (and NICS(1)) values for parent octadehydro[12]annulene are calculated to be +9.20 (+8.10). The NICS(0) (and NICS(1)) of 4' are calculated to be +0.14 (+0.13), which are obviously paradoxical values for compounds with macrocyclic diatropicity. Thus, it is considered that the paratropicity of 3 is significantly weak and the diatropicity of 4 is negligible.

Electronic and Electrochemical Properties. In the electronic absorption spectra (Figure 2), the red shifts of the

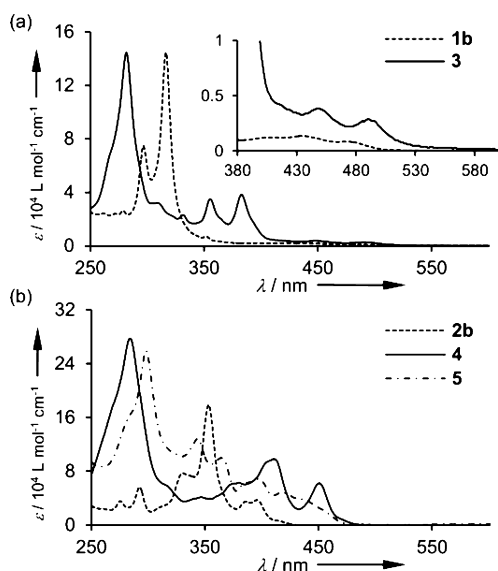


Figure 2. UV-vis spectra of DBAs **1b** and **3** (a) and **2b**, **4**, and **5** (b) in CHCl_3 at 298 K. The data for **3** are plotted with arbitrary intensity because of its instability in the solid state.

longest absorption maxima (λ_{max}) are observed in **3** and **4** compared with **1b** and **2b**, respectively, which are attributed to the extension of π conjugation as a result of the extension of the acetylenic linkages (472 nm (**1b**), 396 nm (**2b**), 490 nm (**3**), and 451 nm (**4**)).^{17,18} Notably, the λ_{max} and absorption onsets are red shifted from **5** and **4** to **3** in spite of **3** having the smallest ring size. Considering that the paratropicity of **3** is significantly weak and the conjugation pathway of **3** is shorter than that of **4** and **5**, the smaller HOMO–LUMO gap of **3** compared to **4** and **5** may derive from the strained acetylenic linkages in **3**.¹⁹ The blue-shifted λ_{max} (418 nm) and absorption onset in **5** relative to **3** and **4** is readily explained by the considerable nonplanarity of **5**, which should suppress the π conjugation to some extent in the macrocyclic framework composed of the benzene moieties and tetrayne linkages. DBAs **1b** and **3–5** are nonfluorescent, whereas **2b** is fluorescent with an absolute fluorescence quantum yield of 0.36 in CHCl_3 .

To gain insight into the frontier orbital energy of DBAs **3–5** as well as **1b** and **2b**, CV analysis in *o*-dichlorobenzene was conducted (Table 1). All of the DBAs displayed amphoteric behavior within the available potential window (Figures S4–S8). Both the oxidation onsets ($E_{\text{onset}}^{\text{ox}}$) and reduction onsets ($E_{\text{onset}}^{\text{red}}$) for **3** and **4** are positively shifted as compared to those for **1b** and **2b**, respectively, reflecting the stronger electron-withdrawing ability of a tetrayne unit compared to that of a diyne unit.²⁰ The $E_{\text{onset}}^{\text{red}}$ values are more positively shifted than the $E_{\text{onset}}^{\text{ox}}$ values; hence, **3** and **4** have smaller potential differences (ΔE_{redox}) between the $E_{\text{onset}}^{\text{ox}}$ and $E_{\text{onset}}^{\text{red}}$ values (namely, the electrochemical HOMO–LUMO gaps) compared

Table 1. Oxidation and Reduction Potentials of DBAs **1b**, **2b**, **3**, **4**, and **5** by CV in *o*-Dichlorobenzene^a and Theoretically Calculated HOMO and LUMO Levels and their Gaps (ΔE_{calcd})^b

	$E_{\text{onset}}^{\text{ox}}$ (E_{pa}) (V)	$E_{\text{onset}}^{\text{red}}$ (E_{pc}) (V)	ΔE_{redox} (V) ^c	HOMO (eV)	LUMO (eV)	ΔE_{calcd} (eV)
1b	+0.63 (+0.78) ^d (+1.21) ^d	−1.99 (−2.16) ^e (−2.51) ^f	2.62	−5.08	−2.29	2.79
2b	+0.82 (+0.96) ^f	−2.17 (−2.43) ^f	2.99	−5.24	−1.96	3.28
3	+0.82 (+0.92) ^d (+1.14) ^d	−1.70 (−1.81) ^e (−1.99) ^f	2.52	−5.28	−2.84	2.44
4	+0.92 (+1.03) ^f	−1.76 (−1.99) ^f	2.68	−5.40	−2.66	2.74
5	+0.95 (+1.05) ^f	−1.81 ^g	2.76	−5.72	−2.79	2.93

^a0.1 mol L^{−1} *n*-Bu₄NPF₆. All potentials are given versus the Fc⁺/Fc couple used as an external standard. Scan rate: 100 mV s^{−1}. ^bB3LYP/6-31+G**//B3LYP/6-31G* for **1'–5'**, where the butoxy groups in **1b**, **2b**, **3**, **4**, and **5** are replaced with methoxy groups. ^cThe electrochemical gap, ΔE_{redox} , is defined as the potential difference between $E_{\text{onset}}^{\text{ox}}$ and $E_{\text{onset}}^{\text{red}}$. ^dReversible wave. ^eQuasi-reversible wave. ^fIrreversible wave. ^gUnresolved wave.

to those of **1b** and **2b**, respectively. The electrochemical HOMO–LUMO gaps become apparently small from **5** and **4** to **3**, as expected from the absorption spectra. These trends are well reproduced by the calculations; the ΔE_{redox} values for **1b**, **2b**, and **3–5** match the calculated gaps (ΔE_{calcd}) for corresponding **1'–5'**.

Self-Association. Unexpectedly, the ¹H NMR spectra of **4** in CDCl₃ showed subtle but distinctive upfield shifts of the aromatic protons upon increasing the concentration (Figure 3a). This indicates the occurrence of self-association in solution

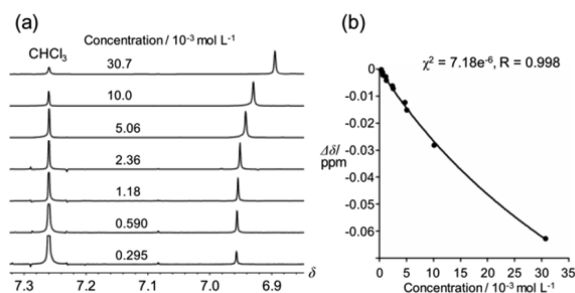


Figure 3. (a) ¹H NMR spectra of **4** in various concentrations of CDCl_3 at 298 K. (b) Nonlinear curve-fitting plots of the concentration dependence of the chemical shifts for aromatic protons of **4**.

by π – π stacking interactions. The diffusion coefficients, *D*, for **4** were almost independent of the concentrations on the basis of the diffusion NMR experiments, suggesting that a monomer–dimer equilibrium predominantly exists.²¹ A plot of the chemical shifts of the aromatic protons as a function of concentration was fitted to a curve for the monomer–dimer model (Figure 3b)²² and yielded the self-association constant (*K_s*) of 4 ± 1 L mol^{−1}. In contrast to **4**, the resonance for the aromatic protons in **2b** was independent of the concentration in CDCl_3 . These results demonstrate that the extension of the acetylenic linkages from **2b** to **4** enhances the self-association ability. To investigate the effect of solvent polarity on the self-

association of **4**, we performed the NMR experiments in the CDCl₃/CD₃CN solvent system. The K_a values in CDCl₃/CD₃CN ratios of 2:1 and 1:1 were 56 ± 5 and 112 ± 45 L mol⁻¹, respectively (Figure S16 in the Supporting Information), which indicate that the self-association is enhanced by the solvophobic effects in the mixed-solvent system.

To examine the electronic effect of the acetylenic linkages on the self-association, we calculated the electrostatic-potential surfaces (ESPs) and molecular electrostatic potentials (MEPs) of **2'** and **4'** at the B3LYP/6-31+G**//B3LYP/6-31G* level (Figure 4). The MEPs at 2 Å above the center of the benzene

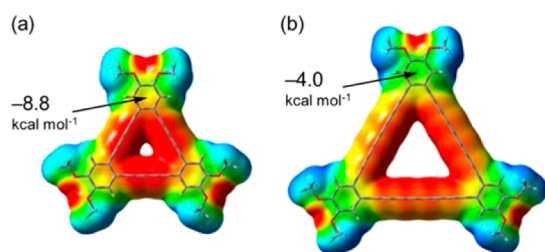


Figure 4. Electrostatic-potential surfaces and values of the molecular electrostatic potentials (MEPs; the calculated position of the MEP is 2 Å above the center of the benzene ring) of **2'** (a) and **4'** (b) at the level of B3LYP/6-31+G**//B3LYP/6-31G*. The potentials are drawn in the same color scale, with red indicating more-negative electrostatic potentials and blue, more-positive potentials.

rings are -8.8 and -4.0 kcal mol⁻¹ for **2'** and **4'**, respectively, which clearly indicates a less-negative character for the benzene rings of **4** than **2b**. It has been widely accepted that electron-withdrawing aromatic rings favor effective π - π stacking interactions.²³ Again, it was pointed out by Tobe and co-workers that arylene-butadiynylene macrocycles possess a higher self-association ability than arylene-ethynylene macrocycles because of the strong electron-withdrawing effect of the butadiyne units in the former.²⁴ Therefore, it is reasonable to conclude that the tetrayne linkages in **4** promote π - π stacking interactions effectively owing to their strong electron-withdrawing effect.

CONCLUSIONS

We have synthesized hitherto unknown [20]-, [30]-, and [40]DBAs **3**–**5** possessing tetrayne linkages. The unique 2D sheetlike network of (DBA **4**)₂(*p*-xylene)₅ in the solid state was revealed. The expansion of the DBA cores by extension of the acetylenic linkages from a diyne to a tetrayne unit significantly decreases tropicity; thus, the paratropicity of **3** should be extremely weak, and the diatropicity of **4** should be negligible. The tetrayne linkages are responsible for small HOMO–LUMO gaps compared to those with diyne linkages. The effective self-association properties of **4** in solution suggest that tetrayne linkages facilitate π - π stacking interactions. Further exploration of the synthesis of novel dehydroannulenes having tetrayne linkages is currently underway in our group.

EXPERIMENTAL SECTION

Preparation of 7. To a solution of **6** (800 mg, 1.93 mmol) in THF/MeOH (1:1, 10 mL) was added K₂CO₃ (528 mg, 3.82 mmol). After the mixture was stirred at room temperature for 50 min, the suspension was evaporated under reduced pressure. The residue was purified by silica gel column chromatography (acetone) to give desilylated diyne, which was used in the next reaction without further purification because of the instability. To a solution of the diyne in

acetone (10 mL) were added *N*-bromosuccinimide (784 mg, 4.40 mmol) and AgNO₃ (96 mg, 0.57 mmol). After the mixture was stirred at room temperature for 6 h, the suspension was evaporated under reduced pressure. The residue was suspended with hexane and filtered, and the filtrate was evaporated under reduced pressure. The residue was purified by silica gel column chromatography (hexane/CH₂Cl₂, 10:1) to afford **7** (430 mg, 1.00 mmol, 52%) as a red solid. mp 64–66 °C. ¹H NMR (CDCl₃, 300 MHz) δ 0.97 (t, 6H, $J = 7.4$ Hz), 1.48 (tq, 4H, $J = 7.4, 7.2$ Hz), 1.78 (tt, 4H, $J = 7.2, 6.8$ Hz), 3.95 (t, 4H, $J = 6.8$ Hz), 6.86 (s, 2H). ¹³C NMR (CDCl₃, 75 MHz) δ 13.8, 19.2, 31.1, 51.9, 68.8, 78.6, 116.1, 118.4, 149.2. UV–vis (CH₂Cl₂) $\lambda_{\max} = 290$ nm. MALDI–TOF MS (Dith, positive) $[M + Na]^+$ 451.00. Anal. Calcd for C₁₈H₂₀Br₂O₂: C, 50.49; H, 4.71. Found: C, 50.03; H, 4.71.

Preparation of 8. To a suspension of CuCl (50 mg, 0.5 mmol) and *n*-BuNH₂ (3.6 mL, 35 mmol) in water (5 mL) and CH₂Cl₂ (5 mL) was added NH₂OH·HCl (5 mg, 0.1 mmol) at 0 °C. A solution of **7** (430 mg, 1.00 mmol) and trimethylsilylacetylene (0.42 mL, 3.00 mmol) in CH₂Cl₂ (2 mL) was added dropwise to the mixture at 0 °C. After the resulting mixture was stirred at 0 °C for 40 min, aqueous NH₄Cl (10%, 30 mL) was added. The organic phase was successively washed with aqueous NH₄Cl (10%, 30 mL) and water (20 mL \times 2), dried over anhydrous MgSO₄, and evaporated under reduced pressure. The residue was purified by silica gel column chromatography (hexane/CH₂Cl₂, 5:1) and recycling GPC (CHCl₃) to afford **8** (130 mg, 0.28 mmol, 28%) as yellow oil. ¹H NMR (CDCl₃, 300 MHz) δ 0.24 (s, 18H), 0.97 (t, 6H, $J = 7.4$ Hz), 1.43–1.51 (m, 4H), 1.79 (tt, 4H, $J = 6.8, 6.8$ Hz), 3.96 (t, 4H, $J = 6.8$ Hz), 6.90 (s, 2H). ¹³C NMR (CDCl₃, 125 MHz) δ -0.2, 13.9, 19.2, 31.0, 68.9, 75.2, 76.8, 88.2, 91.8, 116.9, 117.9, 149.9. UV–vis (CHCl₃) λ_{\max} (rel. int.) = 255 (0.31), 270 (0.60), 286 (1.00), 329 (0.35), 352 (0.36) nm. MALDI–TOF MS (Dith, positive) (M⁺) 462.58. Anal. Calcd for C₂₈H₃₈O₂Si₂·0.04 CHCl₃: C, 72.03; H, 8.20. Found: C, 71.78; H, 7.85.

Preparation of DBAs 3 and 4 (Cu-Mediated Method). A mixture of **8** (656 mg, 1.42 mmol) and K₂CO₃ (392 mg, 2.84 mmol) in THF/MeOH (1:1, 10 mL) was stirred at room temperature for 1 h. After the mixture was diluted with acetone (20 mL), the insoluble material was removed by filtration, and the filtrate was evaporated under reduced pressure. The residue was purified by silica gel column chromatography (acetone) to give desilylated alkyne, which was used in the next coupling reaction without further purification because of the instability. To a mixture of the desilylated alkyne and TMEDA (1.0 mL, 7.10 mmol) in acetone (250 mL) was added CuCl (700 mg, 7.10 mmol) at -5 °C, and the resulting mixture was stirred at room temperature for 22 h. The mixture was filtered through a bed of silica gel, and the filtrate was evaporated under reduced pressure to ca. 1 mL. The mixture was purified by silica gel column chromatography (hexane/toluene, 1:1) to afford unstable [20]DBA **3** and [30]DBA **4** (22 mg, 0.023 mmol, 5%) as yellow solids. [20]DBA **3** decomposed upon concentration to give an insoluble black material. A dilute solution of **3** can be stored for over a year at -15 °C. **3**: ¹H NMR (CDCl₃, 600 MHz) δ 0.96 (t, 12H, $J = 7.3$ Hz), 1.45 (tq, 8H, $J = 7.3, 7.3$ Hz), 1.76 (tt, 8H, $J = 7.3, 6.9$ Hz), 3.91 (t, 8H, 6.9 Hz), 6.62 (s, 4H). ¹³C NMR (CDCl₃, 150 MHz) δ 13.9, 19.2, 31.0, 67.7, 69.0, 70.8, 80.3, 82.2, 114.0, 122.0, 150.5. UV–vis (CHCl₃) λ_{\max} (rel. int.) = 490 (0.02), 447 (0.03), 383 (0.27), 356 (0.24), 332 (0.16), 309 (0.22), 282 (1.00) nm. HR–FAB MS (NBA, positive) m/z (M⁺) calcd for C₄₄H₄₀O₄⁺, 632.2927; found, 632.2927. **4**: mp 155 °C (decomp.). ¹H NMR (CDCl₃, 2.53 \times 10⁻³ L⁻¹ mol, 500 MHz) δ 0.98 (t, 18H, $J = 7.5$ Hz), 1.50 (tq, 12H, $J = 7.5, 7.3$ Hz), 1.81 (tt, 12H, $J = 7.3, 6.8$ Hz), 4.00 (t, 12H, $J = 6.8$ Hz), 6.95 (s, 6H). ¹³C NMR (CDCl₃, 125 MHz) δ 13.9, 19.2, 31.0, 64.4, 68.93, 69.04, 75.7, 77.6, 116.5, 118.3, 150.4. UV–vis (CHCl₃) λ_{\max} (ϵ) = 451 (62 200), 411 (98 100), 380 (62 600), 347 (41 200), 284 (277 300) nm. HR–FAB MS (NBA, positive) m/z (M⁺) calcd for C₆₆H₆₀O₆⁺, 948.4390; found, 948.4380.

Preparation of DBAs 4 and 5 (Pd-Catalyzed Method). Compound **8** (322 mg, 0.88 mmol) was desilylated according to the same procedure used for the preparation of DBAs **3** and **4**. A solution of the desilylated alkyne in Et₃N/THF (1:2, 90 mL) was bubbled with argon with stirring for 30 min. [PdCl₂(PPh₃)₂] (62 mg, 0.088 mmol), CuI (34 mg, 0.176 mmol), and *p*-benzoquinone (85 mg, 0.79 mmol)

were added to the solution, and the resulting mixture was stirred at room temperature for 16 h under argon atmosphere. The mixture was filtered through a bed of silica gel, and the filtrate was evaporated under reduced pressure. The residue was subjected to silica gel column chromatography (CHCl_3). The collected material was suspended with CH_2Cl_2 , and the insoluble material was collected by filtration, which was further washed with CH_2Cl_2 to afford [40]DBA 5 (16 mg, 0.013 mmol, 6%) as a yellow solid. An analytical sample was obtained by reprecipitation from CHCl_3 /hexane. The filtrate was concentrated under reduced pressure. The residue was further purified by recycling GPC (CHCl_3) to afford [30]DBA 4 (18 mg, 0.019 mmol, 7%). 5: mp 148 °C (decomp.). ^1H NMR (CDCl_3 , 600 MHz) δ 0.97 (t, 24H, $J = 7.3$ Hz), 1.41–1.52 (m, 16H), 1.80 (tt, 16H, $J = 6.4, 6.4$ Hz), 3.99 (t, 16H, $J = 6.4$ Hz), 6.92 (s, 8H). ^{13}C NMR (CDCl_3 , 125 MHz) δ 13.9, 19.2, 31.0, 64.5, 68.9, 69.1, 76.0, 77.7, 116.8, 118.3, 150.5. UV–vis (CHCl_3) λ_{max} (ϵ) = 418 (48 400), 397 (68 200), 364 (99 700), 343 (128 300), 298 (259 100) nm. MALDI–TOF MS (SA, positive) $[M + \text{H}]^+$ 1273.87. Anal. Calcd for $\text{C}_{88}\text{H}_{80}\text{O}_8 \cdot 0.29 \text{CHCl}_3$: C, 81.55; H, 6.22. Found: C, 81.55; H, 6.39. We were unable to obtain satisfactory elemental analysis for this compound. This compound may tend to contain solvent molecules in the solid state. We believe that the compound is pure on the basis of the ^1H NMR spectrum.

■ ASSOCIATED CONTENT

■ Supporting Information

General experimental methods, X-ray data (including a CIF file), electrochemistry, theoretical data, self-association properties, and ^1H and ^{13}C NMR spectra of all new compounds. This material is available free of charge via the Internet at <http://pubs.acs.org>.

■ AUTHOR INFORMATION

Corresponding Author

*E-mail: nakamura@gunma-u.ac.jp. Tel: +81 277 30 1310. Fax: +81 277 30 1314.

Notes

The authors declare no competing financial interest.

■ ACKNOWLEDGMENTS

This work was supported by a Grant-in-Aid for Scientific Research from the Ministry of Education, Culture, Sports, Science and Technology, Japan and the Japan Prize Foundation. We thank Dr. Mikio Yamasaki (Rigaku) and Dr. Akihiro Tsurusaki (Gunma University) for X-ray analysis, Dr. Yoshihito Shiota (Kyushu University) for helpful suggestions on the theoretical calculations, and Dr. Keisuke Tao and Prof. Teruo Shinmyozu (Kyushu University) for MALDI–TOF MS measurements.

■ REFERENCES

- (1) (a) Sondheimer, F. *Acc. Chem. Res.* **1972**, *5*, 81. (b) Sondheimer, F. *Chimia* **1974**, *28*, 163. (c) Nakagawa, M. *Pure Appl. Chem.* **1975**, *44*, 885.
- (2) For recent reviews, see (a) Hisaki, I.; Sonoda, M.; Tobe, Y. *Eur. J. Org. Chem.* **2006**, 833. (b) Spilner, E. L.; Johnson, C. A., II; Haley, M. M. *Chem. Rev.* **2006**, *106*, 5344.
- (3) (a) Eglinton, G.; Galbraith, A. R. *Proc. Chem. Soc.* **1957**, 350. (b) Matzger, A. J.; Vollhardt, K. P. C. *Tetrahedron Lett.* **1998**, *39*, 6791. (c) Bunz, U. H. F.; Enlelmann, V. *Chem.—Eur. J.* **1999**, *5*, 263.
- (4) (a) Haley, M. M.; Pak, J. J.; Brand, S. C. *Angew. Chem., Int. Ed. Engl.* **1997**, *36*, 836. (b) Wan, W. B.; Brand, S. C.; Pak, J. J.; Haley, M. M. *Chem.—Eur. J.* **2000**, *6*, 2044.
- (5) Inter alia: (a) Gallagher, M. E.; Anthony, J. E. *Tetrahedron Lett.* **2001**, *42*, 7533. (b) Marsden, J. A.; Haley, M. M. *J. Org. Chem.* **2005**, *70*, 10213. (c) Marsden, J. A.; Miller, J. J.; Shirtcliff, L. D.; Haley, M. M. *J. Am. Chem. Soc.* **2005**, *127*, 2464.
- (6) (a) Wan, W. B.; Kimball, D. B.; Haley, M. M. *Tetrahedron Lett.* **1998**, *39*, 6795. (b) Bell, M. L.; Chiechi, R. C.; Johnson, C. A.; Kimball, D. B.; Matzger, A. J.; Wan, W. B.; Weakley, T. J. R.; Haley, M. M. *Tetrahedron* **2001**, *57*, 3507. (c) Wan, W. B.; Chiechi, R. C.; Weakley, T. J. R.; Haley, M. M. *Eur. J. Org. Chem.* **2001**, 3485.
- (7) (a) Tobe, Y.; Ohki, I.; Sonoda, M.; Niino, H.; Sato, T.; Wakabayashi, T. *J. Am. Chem. Soc.* **2003**, *125*, 5614. (b) Hisaki, I.; Eda, T.; Sonoda, M.; Niino, H.; Sato, T.; Wakabayashi, T.; Tobe, Y. *J. Org. Chem.* **2005**, *70*, 1853.
- (8) Kivala, M.; Mitzel, F.; Boudon, C.; Gisselbrecht, J.-P.; Seiler, P.; Gross, M.; Diederich, F. *Chem.—Asian J.* **2006**, *1*, 479.
- (9) (a) Wegner, G. *Macromol. Chem.* **1972**, *154*, 35. (b) Wegner, G. *Angew. Chem., Int. Ed. Engl.* **1981**, *26*, 361.
- (10) For selected examples of stable polyynes, see (a) Gibtner, T.; Hampel, F.; Gisselbrecht, J.-P.; Hirsch, A. *Chem.—Eur. J.* **2002**, *8*, 408. (b) Zheng, Q.; Gladysz, J. A. *J. Am. Chem. Soc.* **2005**, *127*, 10508. (c) Chalifoux, W. A.; Tykwinski, R. R. *Nat. Chem.* **2010**, *2*, 967.
- (11) Tahara, K.; Johnson, C. A., II; Fujita, T.; Sonoda, M.; De Schryver, F. C.; De Feyter, S.; Haley, M. M.; Tobe, Y. *Langmuir* **2007**, *23*, 10190.
- (12) Kato, S.-i.; Takahashi, N.; Tanaka, H.; Kobayashi, A.; Yoshihara, T.; Tobita, S.; Yamanobe, T.; Uehara, H.; Nakamura, Y. *Chem.—Eur. J.* DOI: 10.1002/chem.201301262, in press.
- (13) All calculations were carried out using Frisch, M. J.; Trucks, G. W.; Schlegel, H. B.; Scuseria, G. E.; Robb, M. A.; Cheeseman, J. R.; Scalmani, G.; Barone, V.; Mennucci, B.; Petersson, G. A.; Nakatsuji, H.; Caricato, M.; Li, X.; Hratchian, H. P.; Izmaylov, A. F.; Bloino, J.; Zheng, G.; Sonnenberg, J. L.; Hada, M.; Ehara, M.; Toyota, K.; Fukuda, R.; Hasegawa, J.; Ishida, M.; Nakajima, T.; Honda, Y.; Kitao, O.; Nakai, H.; Vreven, T.; Montgomery, Jr., J. A.; Peralta, J. E.; Ogliaro, F.; Bearpark, M.; Heyd, J. J.; Brothers, E.; Kudin, K. N.; Staroverov, V. N.; Keith, T.; Kobayashi, R.; Normand, J.; Raghavachari, K.; Rendell, A.; Burant, J. C.; Iyengar, S. S.; Tomasi, J.; Cossi, M.; Rega, N.; Millam, J. M.; Klene, M.; Knox, J. E.; Cross, J. B.; Bakken, V.; Adamo, C.; Jaramillo, J.; Gomperts, R.; Stratmann, R. E.; Yazyev, O.; Austin, A. J.; Cammi, R.; Pomelli, C.; Ochterski, J. W.; Martin, R. L.; Morokuma, K.; Zakrzewski, V. G.; Voth, G. A.; Salvador, P.; Dannenberg, J. J.; Dapprich, S.; Daniels, A. D.; Farkas, O.; Foresman, J. B.; Ortiz, J. V.; Cioslowski, J.; Fox, D. *Gaussian 09*, revision B.01; Gaussian, Inc.: Wallingford, CT, 2010.
- (14) Spantulescu, A.; Luu, T.; Zhao, Y.; McDonald, R.; Tykwinski, R. R. *Org. Lett.* **2008**, *10*, 609.
- (15) For discussion of the crystal packing, see the Supporting Information (Figure S3).
- (16) The NICS value has been successfully used as a measure of tropicity. See von Rague Schleyer, P.; Maerker, C.; Dransfeld, A.; Jiao, H.; van Eikema Hommes, N. J. R. *J. Am. Chem. Soc.* **1996**, *118*, 6317.
- (17) The concentration of CHCl_3 solution for **1b**, **2b**, **4**, and **5** was 10^{-5} – 10^{-6} mol L^{-1} . No deviation from the Lambert–Beer law was observed for **4**, indicating that the self-association of **4** is negligible within the studied concentration range.
- (18) For the assignment of the longer-wavelength absorption in the UV–vis spectra of **1**–**4**, see the Supporting Information.
- (19) It was recently reported that the strain of macrocyclic π systems reduces the HOMO–LUMO gaps. See Sprafke, J. K.; Kondratuk, D. V.; Wykes, M.; Thompson, A. L.; Hoffmann, M.; Drevinskas, R.; Chen, W.-H.; Yong, C. K.; Kärnbratt, J.; Bullock, J. E.; Malfois, M.; Wasielewski, M. R.; Albinsson, B.; Herz, L. M.; Zigmantas, D.; Beljonne, D.; Anderson, H. L. *J. Am. Chem. Soc.* **2011**, *133*, 17262.
- (20) Gisselbrecht, J.-P.; Moonen, N. N. P.; Boudon, C.; Nielsen, M. B.; Diederich, F.; Gross, M. *Eur. J. Org. Chem.* **2004**, 2959.
- (21) Dobrawa, R.; Lysetska, M.; Ballester, P.; Grüne, M.; Würthner, F. *Macromolecules* **2005**, *38*, 1315.
- (22) Martin, R. B. *Chem. Rev.* **1996**, *96*, 3043.
- (23) For reviews of aromatic interactions, see (a) Hunter, C. A.; Lawson, K. R.; Perkins, J.; Urch, C. J. *J. Chem. Soc., Perkin Trans. 2* **2001**, 651. (b) Salonen, L. M.; Ellermann, M.; Diederich, F. *Angew. Chem., Int. Ed.* **2011**, *50*, 4808.

(24) Tobe, Y.; Utsumi, N.; Kawabata, K.; Nagano, A.; Adachi, K.; Araki, S.; Sonoda, M.; Hirose, K.; Naemura, K. *J. Am. Chem. Soc.* **2002**, *124*, 5350.